

Production of the 1S_0 diproton in the $pp \rightarrow pp\pi^0$ reaction at 0.8 GeV

S. Dymov^a, M. Büscher^b, D. Gusev^a, M. Hartmann^b, V. Hejny^b, A. Kacharava^{c,d}, A. Khoukaz^e,
V. Komarov^a, P. Kulesa^f, A. Kulikov^a, V. Kurbatov^a, N. Lang^e, G. Macharashvili^{a,d},
T. Mersmann^e, S. Merzliakov^{a,b}, S. Mikirtychiants^g, A. Mussgiller^b, D. Prasuhn^b, F. Rathmann^b,
R. Schleichert^b, H. Ströher^b, Yu. Uzikov^a, C. Wilkin^{h,*}, S. Yaschenko^{c,a}

^a Laboratory of Nuclear Problems, Joint Institute for Nuclear Research, 141980 Dubna, Russia

^b Institut für Kernphysik, Forschungszentrum Jülich, 52425 Jülich, Germany

^c Physikalisches Institut II, Universität Erlangen–Nürnberg, 91058 Erlangen, Germany

^d High Energy Physics Institute, Tbilisi State University, 0186 Tbilisi, Georgia

^e Institut für Kernphysik, Universität Münster, 48149 Münster, Germany

^f Institute of Nuclear Physics, 31342 Cracow, Poland

^g St. Petersburg Nuclear Physics Institute, 188350 Gatchina, Russia

^h Physics and Astronomy Department, UCL, London, WC1E 6BT, UK

Received 22 December 2005; received in revised form 24 February 2006; accepted 6 March 2006

Available online 20 March 2006

Editor: D.F. Geesaman

Abstract

The $pp \rightarrow pp\pi^0$ differential cross section has been measured with the ANKE spectrometer at COSY–Jülich for pion cms angles between 0° and 15.4° at a proton beam energy of 0.8 GeV. The selection of diproton pairs with an excitation energy $E_{pp} < 3$ MeV ensures that the final pp system is dominantly in the spin-singlet 1S_0 state. The kinematics are therefore very similar to those of $pp \rightarrow d\pi^+$ but with different spin and isospin transitions. The cross sections are over two orders of magnitude smaller than those of $pp \rightarrow d\pi^+$ and show a forward dip that is even stronger than that seen at lower energies. The results should provide a crucial extra test of pion production models in nucleon–nucleon collisions. © 2006 Elsevier B.V. All rights reserved.

PACS: 25.40.Ep; 25.40.Qa; 13.60.Le

Keywords: Nuclear reactions $^1H(p, pp)\pi^0$; $E = 0.8$ GeV; Measured $\sigma(E, \theta)$

Single pion production in nucleon–nucleon collisions, $NN \rightarrow NN\pi$, is the first inelastic process that can be used to test our understanding of the underlying meson–baryon dynamics of the NN interaction [1–3]. By far the cleanest reaction to study is $pp \rightarrow d\pi^+$, where the differential cross section and multitude of spin observables that have been measured over the years [4] can confront the different theoretical models.

In contrast, very little was known about the $pp \rightarrow pp\pi^0$ reaction, though the unexpectedly large π^0 production rate observed near threshold [5] led to a flurry of theoretical activity

[6]. Now in cases where the excitation energy E_{pp} of the final protons is very small, due to the Pauli principle, this reaction will excite only the $J^P = 0^+$ (1S_0) diproton state. Despite having kinematics very similar to those of $pp \rightarrow d\pi^+$, this reaction involves different transitions in the NN system and, in particular, the role of the Δ isobar is expected to be much suppressed because the S -wave ΔN intermediate state is forbidden.

Some information on the transitions involved has been extracted from quasi-free pion absorption on ^3He [7]. However, previous measurements of the differential cross sections for $pp \rightarrow \{pp\}_s\pi^0$ have only been carried out up to a beam energy of 425 MeV, with a cut imposed on the excitation energy of $E_{pp} < 3$ MeV [8,9]. This value satisfies the requirement that the spin-singlet S -wave (1S_0) final state, here denoted by $\{pp\}_s$,

* Corresponding author. Tel.: +44 20 8904 3372.
E-mail address: cw@hep.ucl.ac.uk (C. Wilkin).

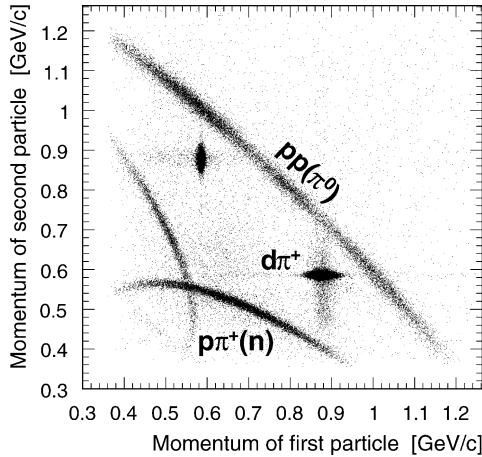


Fig. 1. Scatter plot of the magnitudes of the momenta of two charged particles detected in the FD. The selection procedure introduces a slight bias as to which particle is called “1”, but this does not affect the subsequent analysis.

should dominate while providing reasonable statistics. One important feature of the experimental data is that with the E_{pp} selection the cross sections show a forward dip whereas, if no cut is applied on the excitation energy, then for the higher beam energies there is a forward maximum [9,10].

The threshold for $N\Delta$ production is well above 425 MeV and the data show no sign of being influenced in any clear way by the Δ . We need to go to higher energies to investigate the effects of P -wave ΔN systems. As part of a programme to study the small E_{pp} region in intermediate energy nuclear reactions, in particular in large momentum transfer deuteron breakup reactions [11,12], we have carried out a high statistics measurement of the $pp \rightarrow \{pp\}_s \pi^0$ reaction at $T_p = 800$ MeV for pion cm angles below 15.4° .

The experiment was performed at the magnetic spectrometer ANKE [13], placed at an internal target position of the COSY cooler synchrotron [14]. Fast charged particles, resulting from the interaction of the proton beam with the hydrogen cluster-jet target [15], were registered in the forward detector (FD) system [16]. Its hodoscope provided a trigger signal and an energy-loss measurement. It also allowed a determination of the differences in arrival times for particle pairs hitting different counter elements. The tracking system gave a momentum resolution $\sigma_p/p \approx 0.8\text{--}1.2\%$ for protons in the range (0.5–1.2) GeV/ c .

The trigger used required the crossing of the two planes of the scintillation hodoscopes by at least one charged particle but, in the subsequent off-line analysis of the $pp \rightarrow \{pp\}_s \pi^0$ reaction, only events with two tracks in the FD were retained. In Fig. 1 is shown a two-dimensional scatter plot of the magnitudes of their two momenta corresponding to about half of our statistics. Due to the limited angular acceptance of ANKE, we observe kinematic correlations between the momenta of the registered particles for reactions with two and three particles in the final state. One therefore sees in the figure islands corresponding to $pp \rightarrow d\pi^+$ and bands resulting from $pp \rightarrow pn\pi^+$ and $pp \rightarrow pp\pi^0$. Candidates for the latter reaction are well separated from the other processes. Furthermore, in approximately 75% of cases the particles hit different counters in

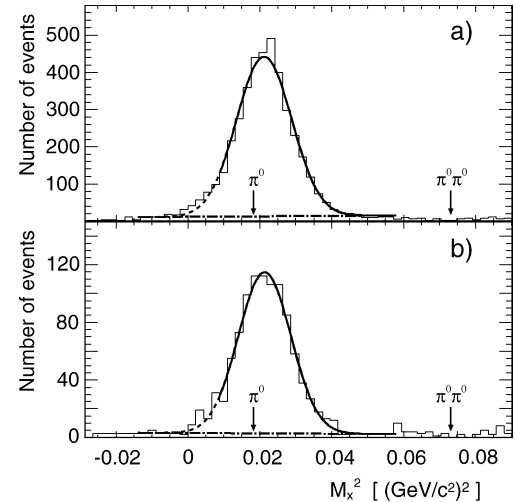


Fig. 2. Distributions in the square of the missing mass for candidates for the $pp \rightarrow ppX$ reaction with excitation energy $E_{pp} < 3$ MeV and $\theta_{pp}^{cm} \leq 15.4^\circ$ when the protons (a) hit different counters, and (b) the same counter. From the indicated positions of the π^0 peak and the $2\pi^0$ threshold it is seen that single and double pion production can be clearly separated. Gaussian fits to the π^0 peak plus a constant background yield a total number of π^0 events in (a) and (b) of respectively 4425 and 1008.

the hodoscope and the difference in their arrival time could also be used in the selection. The $d\pi^+$ pairs coming from the $pp \rightarrow d\pi^+$ reaction, which could potentially provide the most serious physical background, are separated from the pp pairs from $pp \rightarrow pp\pi^0$ in time difference by more than at 8 ns, whereas the actual resolution is better than 0.5 ns.

The distributions of missing mass squared, M_X^2 , are shown separately in Fig. 2 for single-counter and double-counter candidates with low excitation energy in the pp system, $E_{pp} < 3$ MeV. In both cases one sees a very clean π^0 peak centred at 0.021 $(\text{GeV}/c^2)^2$, which agrees with $m_{\pi^0}^2$ to well within our experimental precision. The widths of the Gaussian fits are compatible with those obtained from Monte Carlo simulations; the marginally narrower peak in the single-counter data is due to these events generally having a smaller opening angle resulting in the kinematics being slightly better defined. The backgrounds are small and slowly varying and two-pion production can be clearly excluded in either case. There is a small excess of events observed on the left side of the π^0 peak. These may correspond to single photon production through $pp \rightarrow \{pp\}_s \gamma$ and so the regions indicated by dashed lines in Fig. 2 have not been included in the Gaussian fits. Since this interpretation is not unambiguous and these events might still correspond to good π^0 events, we have added an extra 2% to the systematic error. Given that the two data sets are completely compatible, they have been grouped together in the subsequent analysis. The resolution in excitation energy for the combined $pp \rightarrow pp\pi^0$ events was $\sigma(E_{pp}) \approx 0.2\text{--}0.3$ MeV for E_{pp} in the range 0–3 MeV.

The value of the luminosity needed to determine the cross section was found by comparing the yield of pp elastic scattering, measured simultaneously with the other reactions, with that deduced from the SAID data base [17]. The integrated lumi-

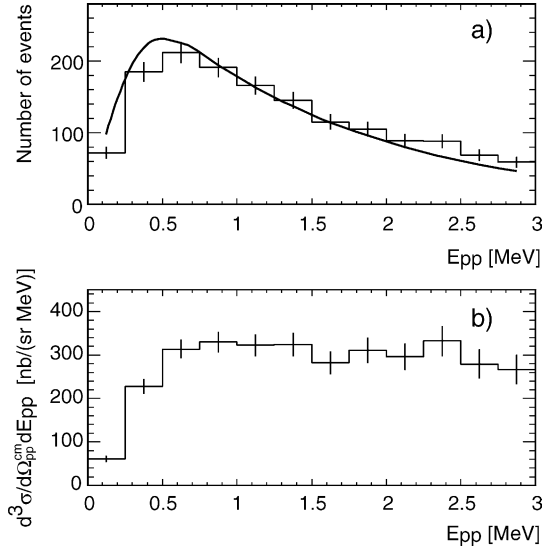


Fig. 3. (a) Number of $pp \rightarrow pp\pi^0$ events in the interval $8.9^\circ < \theta_{pp}^{\text{cm}} < 13^\circ$ as a function of E_{pp} ; (b) The same data corrected for acceptance and detection efficiency and presented as differential cross sections. Only statistical errors are shown. The curve results from passing the Migdal–Watson function $|T(E_{pp})|^2$ of Eq. (1), multiplied by phase space, through a Monte Carlo simulation of the ANKE apparatus and normalising the predictions to the summed experimental histogram. Similar results are found for the other angular intervals.

nosity obtained from this is $L_{\text{int}} = (6.72 \pm 0.26) \times 10^{34} \text{ cm}^{-2}$, where the error comes mainly from averaging over the angular bins.

In order to determine the triply differential cross section $d^3\sigma/(d\Omega_{pp}^{\text{cm}} dE_{pp})$, events selected in the range $0 \leq E_{pp} < 3 \text{ MeV}$ were divided into groups of equal intervals in $\cos\theta_{pp}^{\text{cm}}$, where θ_{pp}^{cm} is the angle of the diproton momentum with respect to the beam direction in the cm system. The energy spectrum of counts in a typical angular interval is shown in Fig. 3(a); the spectra in the other intervals demonstrate a similar behaviour. Values of the corresponding cross sections were obtained from such a distribution by taking into account geometrical acceptance, efficiency in the track recognition algorithm for two particles, interactions in the constituent materials, efficiency and resolution of the detectors and other known effects on the basis of a Monte Carlo simulation of the ANKE setup. This leads to the histogram with the statistical errors presented in Fig. 3(b).

The rapid rise of the spectrum with E_{pp} from threshold illustrated in Fig. 3(b) is typical of all intermediate energy reactions where one produces proton pairs and is induced by the pp final state interaction. We have indeed observed exactly the same phenomenon in the $pd \rightarrow (pp)n$ reaction with the same apparatus at ANKE [11,12]. This effect is often parameterised, in the Migdal–Watson approximation [18], by the square of the low energy pp elastic scattering amplitude for which

$$|T(E_{pp})|^2 = \frac{1}{|C(\eta)|^2} \left(\frac{\sin \delta}{k} \right)^2, \quad (1)$$

where $|C(\eta)|^2$ is the Coulomb penetration factor evaluated at $\eta = \alpha m_p/2k = \alpha \sqrt{m_p/E_{pp}}/2$, and δ is the combined Coulomb–nuclear phase shift. This has been evaluated numer-

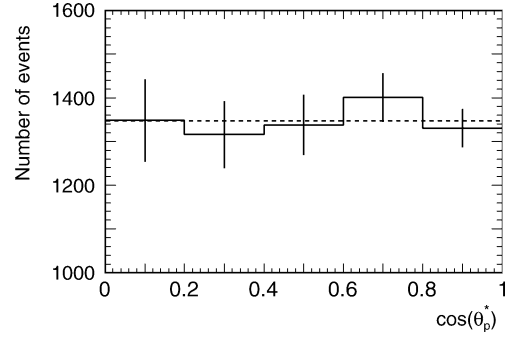


Fig. 4. Distribution of acceptance-corrected $pp \rightarrow \{pp\}_s\pi^0$ events with $E_{pp} < 3 \text{ MeV}$ over $\cos\theta_p^*$, where θ_p^* is the angle between relative pp momentum in the diproton rest frame and the diproton momentum in the overall cm frame. Note that the vertical scale does not start from zero. The resolution in $\cos\theta_p^*$ depends upon the angle but, even in the worst case, it is no larger than the width of the bins.

ically for the Reid soft core potential, for which the scattering length $a_{pp} = -7.8 \text{ fm}$.

The Migdal–Watson factor of Eq. (1) was used as an event generator together with phase space to provide candidates which were then traced through the experimental setup, taking into account all its known features. The resulting smoothed curve, shown in Fig. 3(a), provides a semi-quantitative description of the data which is quite sufficient for our purpose, where we quote cross sections summed over energy. The data are a little above the curves at the higher E_{pp} and we cannot exclude some small P -wave contribution though globally the angular distribution of the pp system in its rest frame shown in Fig. 4 is consistent with isotropy. It should be noted that the 3P_0 final state would also produce a flat distribution.

Due to the identity of the initial protons, the differential cross section is an even function of $\cos\theta_{\pi}^{\text{cm}}$ and in Fig. 5 it is plotted versus $\cos^2\theta_{\pi}^{\text{cm}}$. The resolution in $\cos\theta_{\pi}^{\text{cm}}$, which is always smaller than the bin size, varies from about 0.003 at $\theta_{\pi}^{\text{cm}} = 15^\circ$ down to 0.001 at 0° . The cross section shows a monotonic decrease towards the forward direction and, as seen from the figure, this can be well parameterised by the linear function $a(1 + b \sin^2\theta_{\pi}^{\text{cm}})$, where $a = (704 \pm 22_{\text{stat}} \pm 32_{\text{sys}}) \text{ nb/sr}$ and $b = 5.6 \pm 1.2$. With the same E_{pp} cut as used here, a similar forward dip was observed in this reaction at lower energies, $T_p \leq 425 \text{ MeV}$ [8,9], though for these energies it was found that b was much smaller, being always less than 1.4. Since, for such small values of E_{pp} , the final diproton must be dominantly in an S -wave, constraints from spin–parity and Fermi statistics then require the pion to be in an even partial wave. As a consequence, the forward dip was attributed to an interference between the pion s - and d -waves [9]. Given that the influence of d -waves might be expected to increase with energy, it is perhaps not surprising that we find a larger slope parameter at 800 MeV.

Preliminary theoretical predictions have been made for the $pp \rightarrow \{pp\}_s\pi^0$ differential cross section at 800 MeV in a model that includes contributions from P -wave ΔN intermediate states [19,20]. The overall magnitude is similar to that which we have observed and, in particular, the forward slope, driven by the joint effects of the pion s - and d -waves, is well reproduced. In fact, if the theoretical curve were displaced by a mere

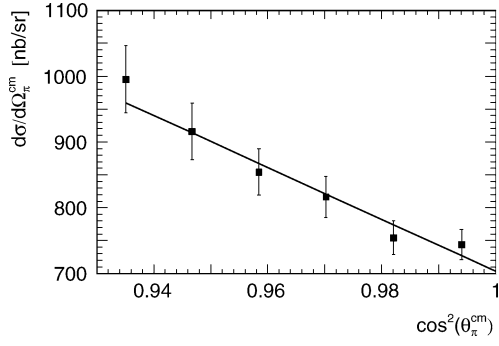


Fig. 5. The measured $pp \rightarrow \{pp\}_s \pi^0$ differential cross section for $E_{pp} < 3$ MeV as a function of $\cos^2(\theta_\pi^{\text{cm}})$. The curve is a straight-line fit to the data.

Table 1

Zero degree differential cross sections for $pp \rightarrow \{pp\}_s \pi^0$ with $E_{pp} < 3$ MeV from the present experiment at 800 MeV with the lower energy data being taken from Ref. [9]. The values of the $pp \rightarrow d\pi^+$ cross sections are obtained from the SAID SP96 solution with the range of the other solutions being taken as a rough estimate of the error bars [17]. The ratio $R(\pi^0/\pi^+)$ of the two pion-production cross sections is also presented

T_p (MeV)	$\sigma(pp\pi^0)$ (nb/sr)	$\sigma(d\pi^+)$ ($\mu\text{b/sr}$)	$R(\pi^0/\pi^+)$ $\times 10^3$
310	109 ± 8	14.1 ± 0.3	7.7 ± 0.6
320	110 ± 6	22.1 ± 0.6	5.0 ± 0.3
340	95 ± 10	41.9 ± 1.5	2.3 ± 0.3
360	86 ± 7	67.1 ± 2.7	1.3 ± 0.1
400	121 ± 9	135 ± 2	0.9 ± 0.1
425	171 ± 14	189 ± 3	0.9 ± 0.1
800	704 ± 22	155 ± 4	4.5 ± 0.4

0.04 in $\cos \theta_\pi^{\text{cm}}$, it would pass through our experimental points. It is expected that our data, combined with those at lower energies, will allow such models to be refined.

Though we have argued that the kinematics of $pp \rightarrow \{pp\}_s \pi^0$ and $pp \rightarrow d\pi^+$ are quite similar, the underlying dynamics must be very different. This is illustrated in Table 1, where we show the values of the two differential cross sections and their ratio $R(\pi^0/\pi^+)$ in the forward direction obtained at different energies. The results seem to indicate that there might be a broad minimum in R in the Δ region of the $pp \rightarrow d\pi^+$ reaction.

The GEM Collaboration has recently published high precision data on the ratio of the forward production of pions in the $pp \rightarrow \pi^+ d$ and $pp \rightarrow \pi^+ pn$ reactions at 981 MeV [21]. Since the spin-singlet pn final state interaction has a much sharper energy dependence than that of the triplet, from the shape of the pion momentum spectrum they could put an upper limit on the amount of pn singlet produced. Integrating over excitation energies $E_{pp} < 3$ MeV, it is seen that the ratio of $\frac{d\sigma}{d\Omega}(pp \rightarrow \{pn\}_s \pi^+)$ to $\frac{d\sigma}{d\Omega}(pp \rightarrow d\pi^+)$ could be at most about 5%. If Coulomb effects are ignored, the cross sections for spin-singlet production through $pp \rightarrow \{pn\}_s \pi^+$ and $pp \rightarrow \{pp\}_s \pi^0$ should be identical. Though Coulomb suppression in the $\{pp\}_s$ final state will be large, it looks very doubtful whether the study of the spectrum alone will be sufficient to isolate the $pp \rightarrow \{pn\}_s \pi^+$ cross section in view of the values

presented in Table 1. Measuring the proton and pion in coincidence, as has been done for example in Refs. [22,23] and analysed in a model-independent way [24], still only provides upper bounds. The study of π^0 production therefore seems to be the most realistic way of investigating the 1S_0 final state here.

Data on quasi-free pion production in the $pd \rightarrow \{pp\}_s X$ reaction were obtained as a by-product of our deuteron breakup measurements [11] and these results will be interpreted in terms of the sum of the cross sections for $pp \rightarrow \{pp\}_s \pi^0$ and $pn \rightarrow \{pp\}_s \pi^-$. At 800 MeV it will then be possible to subtract the π^0 contribution reported here in order to obtain data on π^- production.

It is intriguing to note that a very similar ratio to that of Table 1 has been observed for backward dinucleon production in the $pd \rightarrow \{pp\}_s n$ and $pd \rightarrow dp$ reactions at intermediate energies [11]. Now such a connection would be natural within a one-pion-exchange mechanism, where the large momentum transfer $pd \rightarrow dp$ reaction is driven by a $pp \rightarrow d\pi^+$ subprocess [25,26]. More quantitative estimates of the $pd \rightarrow \{pp\}_s n$ cross section, where the $pp \rightarrow \{pp\}_s \pi^0$ sub-process is used rather than the $pp \rightarrow d\pi^+$, are currently under way [27].

It is seen from Table 1 that there is a real lack of data on the $pp \rightarrow \{pp\}_s \pi^0$ reaction in the Δ region and this could be usefully filled by further experiments at ANKE. It should also be noted that, unlike the complicated spin structure connected with the $pp \rightarrow d\pi^+$ reaction, only two spin amplitudes which are functions of $\cos^2 \theta_\pi$ are required to describe the $pp \rightarrow \{pp\}_s \pi^0$ reaction. These can be isolated, up to an unmeasurable overall phase, by determining the proton analysing power and the initial pp spin correlation C_{xx} . Both of these experiments can be carried out at small angles using ANKE [28] and the resulting amplitude analysis will tie down even further πNN dynamics at intermediate energies.

Acknowledgements

This work was supported in part by the BMBF grants ANKE COSY–JINR, Kaz-02/001 and Heisenberg–Landau programme. We are grateful to many other members of the ANKE Collaboration who provided strong support for the measurement. Important discussions with J.A. Niskanen and correspondence with I. Strakovsky are also gratefully acknowledged.

References

- [1] H. Garcilazo, T. Mizutani, πNN Systems, World Scientific, Singapore, 1990.
- [2] H. Machner, J. Haidenbauer, J. Phys. G 25 (1999) R231.
- [3] C. Hanhart, Phys. Rep. 397 (2004) 155.
- [4] R.A. Arndt, et al., Phys. Rev. C 48 (1993) 1926.
- [5] H.O. Meyer, et al., Nucl. Phys. A 539 (1992) 633.
- [6] See for example: T.-S.H. Lee, D.O. Riska, Phys. Rev. Lett. 70 (1993) 2237.
- [7] M.A. Moinester, et al., Phys. Rev. Lett. 52 (1984) 1203.
- [8] Y. Maeda, N. Matsuoka, K. Tamura, Nucl. Phys. A 684 (2001) 392c.
- [9] R. Bilger, et al., Nucl. Phys. A 693 (2001) 633.
- [10] G. Rappenecker, et al., Nucl. Phys. A 590 (1995) 763.
- [11] V. Komarov, et al., Phys. Lett. B 553 (2003) 179.
- [12] S. Yaschenko, et al., Phys. Rev. Lett. 94 (2005) 072304.

- [13] S. Barsov, et al., Nucl. Instrum. Methods A 462 (1997) 364.
- [14] R. Maier, Nucl. Instrum. Methods A 390 (1997) 1.
- [15] A. Khoukaz, et al., Eur. Phys. J. D 5 (1999) 275.
- [16] S. Dymov, et al., Part. Nucl. Lett. 1 (2004) 40.
- [17] SAID data base available from <http://gwdac.phys.gwu.edu>.
- [18] K.M. Watson, Phys. Rev. 88 (1952) 1163;
A.B. Migdal, Sov. Phys. JETP 1 (1955) 2.
- [19] J.A. Niskanen, Phys. Rev. C 43 (1991) 36.
- [20] J.A. Niskanen, in preparation.
- [21] M. Abdel-Bary, et al., Phys. Lett. B 610 (2005) 31.
- [22] J. Hudomalj-Gabitzsch, et al., Phys. Rev. C 18 (1978) 2666.
- [23] V. Abaev, et al., Phys. Lett. B 521 (2001) 158.
- [24] Yu.N. Uzikov, C. Wilkin, Phys. Lett. B 511 (2001) 191.
- [25] N.S. Craigie, C. Wilkin, Nucl. Phys. B 14 (1969) 477.
- [26] V.M. Kolybasov, N.Ya. Smorodinskaya, Yad. Fiz. 17 (1973) 1211.
- [27] Yu.N. Uzikov, C. Wilkin, in preparation.
- [28] A. Kacharava, F. Rathmann, C. Wilkin, nucl-ex/0511028.